Editors' Suggestion

Critical Thickness in Superconducting $LaAlO_3/KTaO_3(111)$ Heterostructures

Yanqiu Sun,[1] Yuan Liu,[1] Siyuan Hong,[1] Zheng Chen,[1] Meng Zhang,[1] and Yanwu Xie[1,2,*]

[1]*Interdisciplinary Center for Quantum Information, State Key Laboratory of Modern Optical Instrumentation, and Zhejiang Province Key Laboratory of Quantum Technology and Device, Department of Physics, Zhejiang University, Hangzhou 310027, China*

[2]*Collaborative Innovation Center of Advanced Microstructures, Nanjing University, Nanjing 210093, China*

(Received 26 April 2021; accepted 29 July 2021; published 19 August 2021)

Recently, two-dimensional superconductivity was discovered at the oxide interface between $KTaO_3$ and $LaAlO_3$ (or EuO), whose superconducting transition temperature T_c is up to 2.2 K and exhibits strong crystalline-orientation dependence. However, the origin of the interfacial electron gas, which becomes superconducting at low temperatures, remains elusive. Taking the $LaAlO_3/KTaO_3(111)$ interface as an example, we have demonstrated that there exists a critical $LaAlO_3$ thickness of ~3 nm. Namely, a thinner $LaAlO_3$ film will give rise to an insulating but not conducting (or superconducting) interface. By *in situ* transport measurements during growth, we have also revealed that the critical thickness can be suppressed if exposure to oxygen is avoided. These observations, together with other control experiments, suggest strongly that the origination of the electron gas is dominated by the electron transfer that is from oxygen vacancies in the $LaAlO_3$ film to the $KTaO_3$ substrate.

DOI: 10.1103/PhysRevLett.127.086804

In 2004, Ohtomo and Hwang [1] discovered that a two-dimensional electron gas (2DEG) can be formed by depositing $LaAlO_3$ (LAO) thin film on TiO_2-terminated $SrTiO_3$ (STO) single-crystal substrates. Later [2], it was found that a minimal LAO thickness of about 3–4 unit cells (~1.2–1.6 nm) is needed for the formation of this 2DEG. This minimal thickness is the so-called critical thickness, which plays a key role in understanding the origin of 2DEG at the LAO/STO interface [3,4]. The existence of such a critical thickness also makes LAO/STO a unique platform in fabricating reversibly sketched nanoelectronics with an atomic force microscope (AFM) tip [5–8].

Very recently, two-dimensional superconductivity, as well as the 2DEG, was discovered at the interfaces between LAO (or EuO) and $KTaO_3$ (KTO) [9–13]. This interface superconductivity is extremely intriguing. First, its superconducting transition temperature (T_c) is up to 2.2 K [9,10,13]. By contrast, superconductivity has never been observed in bulk KTO [14,15] and was reported only at the KTO(001) surface gated by the electric double-layer technique, with an extremely low $T_c \sim 50$ mK [15]. Second, the superconductivity and the T_c depend strongly on the crystalline orientation of KTO single-crystal substrates [9,10]. For the three principal orientations, optimal T_c on KTO(111) and KTO(110) interfaces is ~2.2 K [9,13] and ~0.9 K [10], respectively, while there is no hint of superconductivity at the KTO(001) interface down to 25 mK [9]. Third, given the fact that the electron-doped bulk KTO has never been found to be superconducting [14,15], while the electron-doped STO is superconducting in bulk and has similar T_c as that of the LAO/STO interface [16], the superconductivity observed at KTO interfaces can be thought to be a more intrinsic interface effect than that of the well-known LAO/STO interface. Last but not the least, the superconductivity at KTO interfaces can be strikingly tuned by applying an electric field [13], despite the relatively high carrier density. It is remarkable that the electric gating can modify the carrier mobility quite a lot, although it has only a minor effect on carrier density. To explore these exotic features of intriguing KTO interfaces, the interface conduction mechanism is highly in demand.

In this Letter, taking LAO/KTO(111) as an example, we have studied how interfacial transport properties depend on the LAO thickness. It has been observed that, analogous to the LAO/STO interface, there exists a critical LAO thickness ~3 nm for the LAO/KTO(111) interface. The interface will become conducting (insulating) when LAO is thicker (thinner) than this critical thickness. Exploiting *in situ* transport measurements during growth, we have demonstrated that this critical thickness is closely related to oxygen vacancies in the LAO film and can be suppressed if exposure to oxygen is avoided. These observations suggest that the electron transfer from oxygen vacancies in LAO to the interfacial KTO is the dominant mechanism for the interface conduction.

Our samples were fabricated by depositing LAO films on KTO(111) single-crystal substrates by pulsed laser deposition (PLD). Details can be found in Supplemental Material [17]. If not specified otherwise, the samples were grown under normal conditions: The growth temperature is 680 °C; the growth atmosphere is 1×10^{-5} mbar O_2

(adding a tiny amount of H_2O vapor, 1×10^{-7} mbar) [10,13,17]. AFM characterizations show that the sample surfaces are very smooth, with a root mean square roughness below 0.2 nm (Fig. S1 [17]). X-ray diffraction detects no epitaxial peaks of LAO (Fig. S3 [17]), consistent with previous studies [9,10,12,13] that the LAO film is in an amorphous state.

As shown in Fig. 1, for the interfaces to be conducting, the thickness of LAO, d_{LAO}, has to reach a critical thickness, $d_c \approx 3$ nm. All samples with $d_{\mathrm{LAO}} > \sim 3$ nm are conducting, with a sheet conductance σ_s on the order of $10^{-5} - 10^{-4}\ \Omega^{-1}$ (at ~300 K); all samples with $d_{\mathrm{LAO}} \leq d_c$ are insulating in all the measured temperatures, 300 K and below ($\sigma_s < 1 \times 10^{-8}\ \Omega^{-1}$, the measurement limit). A similar critical thickness was also observed in the LAO/KTO(001) and LAO/KTO(110) interfaces (see Fig. S4 [17]). This observation of critical thickness is very similar to that observed in LAO/STO, in which a $d_c \sim 3$–4 unit cells (~1.2–1.6 nm) was found [2]. However, the nature of the presently observed critical thickness is different. In LAO/STO, the LAO film is epitaxially grown on the STO substrate. The polar discontinuity at the interface and the resulting divergent built-in potential in LAO, which eventually triggers an electronic reconstruction, are the proposed origin [3,4]. In sharp contrast, in LAO/KTO(111), there is no regular polar arrangement of atomic layers in LAO due to its amorphous nature, and, thus, polar-discontinuity and electronic reconstruction is irrelevant. Rather, the situation is apparently like the conducting interfaces between STO and amorphous oxides [18,19].

What is the origin of the present critical thickness, and which information does it provide for the conduction mechanism in LAO/KTO? To address this question, we performed *in situ* transport measurements during growth. We note that such a kind of experiments are difficult to be carried out at high temperatures, because, in addition to technical challenges, complications such as ionic conduction and thermal generation of electron-hole pairs can be involved. To avoid these difficulties, we performed *in situ* experiments at room temperature. We grew 1-nm LAO/KTO(111) samples under normal conditions as the starting ones [named as norm(1 nm) hereafter]. These norm (1 nm) samples are highly insulating, because their LAO layer is thinner than d_c. Then we continued to deposit LAO on them in vacuum at room temperature (RT), during which the transport properties can be monitored with prepositioned electrodes (Fig. S5 [17,20]). As will be discussed below, the initial 1-nm LAO layer grown under normal conditions ensures that the samples used for the *in situ* experiments have a comparable interface with the superconducting samples reported previously [10,13] [note that the interface formed between KTO(111) and LAO deposited under RT conditions shows an inferior superconducting behavior; see Fig. S6 [17]].

We verify first that such prepared samples share the same essential features as the normal ones. In Figs. 2(a) and 2(b), we present the temperature-dependent sheet resistance R_s for a normal sample and a "norm(1 nm) + RT(x nm)" sample [here, RT(x nm) represents that the corresponding LAO layer was grown under RT conditions as described above]. Both samples have a total LAO thickness of 10 nm.

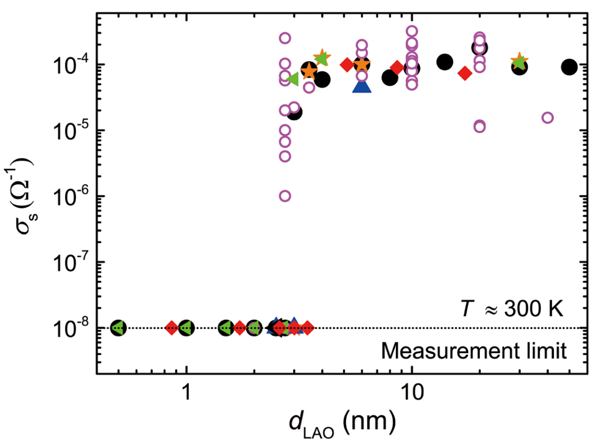

FIG. 1. Influence of LAO thickness d_{LAO} on the transport properties of LAO/KTO(111) interfaces. The solid symbols represent the samples grown under normal conditions. Different symbol shapes are used when more than one sample has been fabricated with the same d_{LAO}. The empty symbols represent the samples grown under other conditions in which the growth temperatures were varied from 100 to 800 °C, and the growth oxygen pressures were varied from 0 to 5×10^{-5} mbar. The data were taken at room temperature, $T \approx 300$ K.

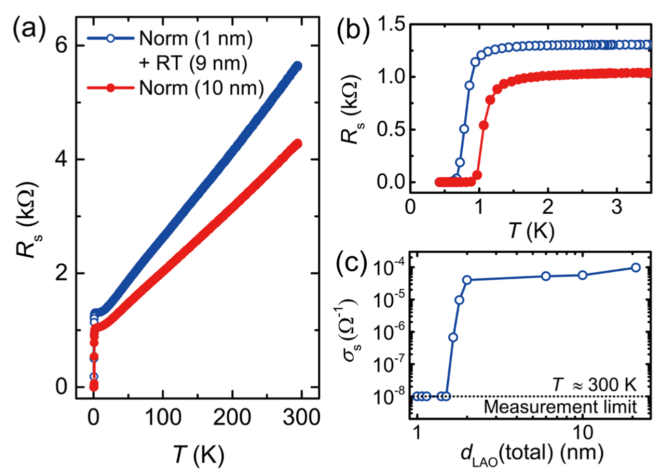

FIG. 2. Comparison of two types of samples. Norm, grown under normal conditions. RT, grown at room temperature in vacuum. (a) Sheet resistance R_s as a function of temperature. (b) A close view of $R_s(T)$ curves in the low-temperature range. (c) Influence of d_{LAO} (total) on the transport properties of LAO/KTO(111) interfaces that were prepared by depositing x-nm LAO at RT on norm(1 nm) or, namely, norm(1 nm) + RT(x nm). Here, $d_{\mathrm{LAO}}(\mathrm{total}) = (1 + x)$ nm.

The two samples exhibit comparable transport behaviors except that the latter has a slightly larger overall R_s and a slightly lower T_c (midpoint) (0.8 vs 1.1 K). Hall effect measurements performed at 10 K show that the 2D carrier density is 1.2×10^{14} and 1.0×10^{14} cm^{-2} for the norm(10 nm) and the norm(1 nm) + RT(9 nm) samples, respectively. Furthermore, as shown in Fig. 2(c), a critical thickness, $d_c \sim 1.6$ nm, was observed for the norm(1 nm) + RT(x nm) samples as well (the dependence of d_c on the thickness of the initial normal LAO can be found in Figs. S7 and S8 [17]). As will be discussed below, the smaller value of d_c can be ascribed to the fact that RT(x nm) was deposited in vacuum (oxygen deficient). In the following, we use norm(1 nm) + RT(x nm) samples for our *in situ* studies.

A typical set of data is presented in Fig. 3(a). The interface conduction changes dramatically from insulating into conducting when even only a single laser pulse shoots. The conductance is quite stable in vacuum, which only decreases slowly with time, and increases gradually with increasing the number of ablation laser pulses, until saturation. However, the conductance decreases sharply when a large amount of oxygen is filled into the growth chamber and cannot recover by further pumping the chamber into vacuum. Finally, when measured *ex situ* in air, this norm(1 nm) + RT(30 pulses = 0.4 nm) sample is fully insulating. This set of data is very informative, showing that the interface conduction is closely related to oxygen vacancies, which are expected for films deposited in vacuum and can be refilled by supplying abundant oxygen.

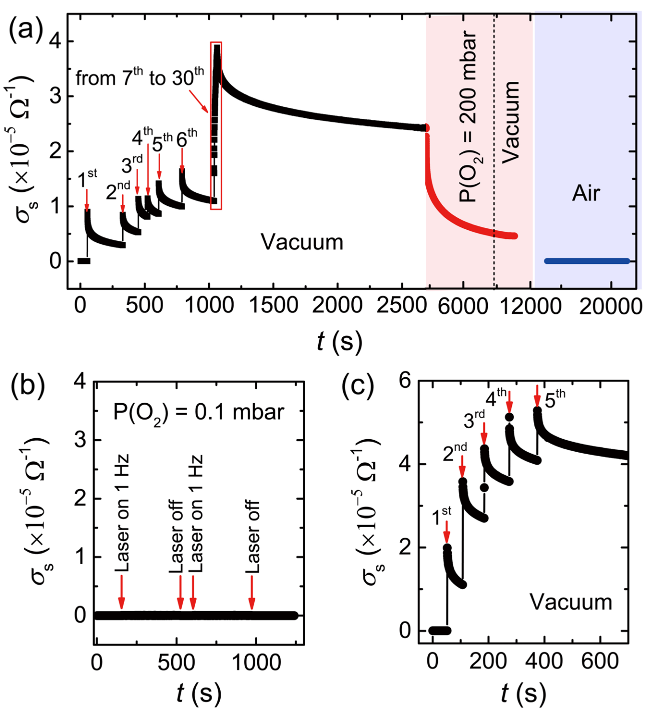

FIG. 3. *In situ* transport measurements for depositing LAO at room temperature on norm(1 nm) samples. (a) Evolution of sheet conductance σ_s with time. The chamber environment in different time zones was as labeled. The red arrows indicate the moment when a laser pulse shoots. Note that the durations of one laser pulse and its induced plume are ~25 ns and ~10 μs, respectively. These two timescales are much shorter than the time interval of acquiring data in our measurements (~0.5 s). Different timescales were used in different time zones. (b) Depositing 10-nm LAO film under $P(O_2) = 0.1$ mbar. (c) Depositing LAO on a norm(1 nm) sample that had been annealed at 400 °C in $P(O_2) =$ 1 bar flow for 24 h. The calibrated growth rate of LAO is ~0.014 nm per laser pulse [17].

As a control experiment, we have also deposited LAO on norm(1 nm) at room temperature under $P(O_2) = 0.1$ mbar rather than in vacuum. As shown in Fig. 3(b), the *in situ* transport measurement shows that in this case the sample is always insulating. This observation further supports that oxygen vacancies, which are absent in samples deposited in the oxygen-rich environment, play a determinant role in the conduction.

Learned from the extensive previous studies [19–26] of LAO/STO, we know that oxygen vacancies can be generated in both the films and the substrates, particularly in those grown under low oxygen pressures. In principle, both kinds of oxygen vacancies can contribute significantly to the interface conduction by supplying electrons. Here, we argue that in the present LAO/KTO(111) the oxygen vacancies in the LAO film play a determinant role. We have annealed a norm(1 nm) sample at 400 °C in $P(O_2) = 1$ bar flow for 24 h. This extreme oxidization process will fill all the oxygen vacancies in both the 1-nm LAO film and the KTO substrate. We then performed the *in situ* transport measurements during further deposition of LAO at room temperature, in vacuum. The result is shown in Fig. 3(c). Clearly, the key result is essentially the same as that of the as-grown norm(1 nm) [Fig. 3(a)]. We point out that the further deposition of LAO will not generate oxygen vacancies in KTO. In LAO/STO, it has been proposed that oxygen vacancies can be generated in the STO substrate by striking of the energetic species in the PLD plume or by interfacial redox reactions [18,20,25,27]. However, coming back to the present case, the 1-nm preexisting LAO layer will impede these two processes in generating oxygen vacancies in the KTO substrate. The diffusion of oxygen vacancies from LAO to KTO is also less likely, because at room temperature the diffusion rate is extremely slow. In addition, we found that the KTO(111) substrate bombarded by Ar ions for 30 min, which should have generated lots of oxygen vacancies in KTO(111), is not metallic (see Fig. S9 [17]). Therefore, we can rule out that the oxygen vacancies in the KTO substrate as the determinant mechanism and take the remaining one: oxygen vacancies in the LAO film.

Thus, a natural scenario for the interface conduction is that oxygen vacancies in LAO supply electrons to the KTO near the interface by charge transfer. Just like in LAO/STO [28], charge transfer will produce an interfacial potential well in KTO, where the conduction electrons locate. By measuring the thickness of the superconducting layer, Liu *et al.* [9] and Chen *et al.* [13] have determined that at low temperatures the width of the potential well in KTO(111) heterostructures is about several nanometers. Certainly, the presence of a charge-transfer-induced potential well can further accumulate electrons from oxygen vacancies in KTO, if there are any. Remember that all the LAO/KTO or EuO/KTO superconducting interfaces [9–11,13] reported until now were fabricated under low oxygen pressure, and, thus, oxygen vacancies are indeed expected in KTO, as well as in LAO or EuO. So, in these samples both oxygen vacancies in LAO and KTO can contribute significantly to the conduction. However, we emphasize that, even in the latter case, the determinant role is still played by the oxygen vacancies in LAO, since they create the potential well. For comparison, we have examined the bare KTO substrates that have experienced all the same growth processes except for the film deposition and found that they are highly insulating (not shown).

With the above scenario in mind, we can explain the critical thickness as the minimal thickness of LAO that can maintain sufficient oxygen vacancies in LAO (particularly in the LAO layer close to the interface) after exposure to ambient environment. That the norm(1 nm) + RT(x nm) samples have a smaller d_c than the normal ones can be understood by that RT(x nm) was deposited in an even more oxygen-deficient environment (in vacuum). Finally, encouraged by the great successes in previous studies of LAO/STO with state-of-the-art tunneling [29] and spectroscopic [30] techniques, one would expect to apply the same techniques to achieve deep insights of the LAO/KTO interfaces. To this end, it is demanded to reduce the d_c of LAO/KTO. We point out that deposition in vacuum is not an ideal way for this purpose, because, although it can reduce d_c [Figs. 2(c) and S7 [17]], the resulting samples are susceptible to ambient environment. Interestingly, we found that the reduction of d_c can be achieved by partly replacing the top LAO layer with Al_2O_3, another highly insulating dielectric. As shown in Fig. 4, it is possible to fabricate robust superconducting KTO(111) interface samples with a reduced total thickness of the insulating films.

In summary, we have demonstrated that there exists a critical thickness of the LAO film in the superconducting LAO/KTO(111) interface. With the help of *in situ* transport measurements during growth, we found that this critical thickness is related to the refilling of oxygen vacancies in the LAO film. These results provide experimental evidence that the interface conduction is dominated by the electron transfer from the oxygen vacancies in LAO to KTO. The existence of this critical thickness in LAO/KTO(111) not only sheds light on the conduction mechanism, but also suggests an attractive

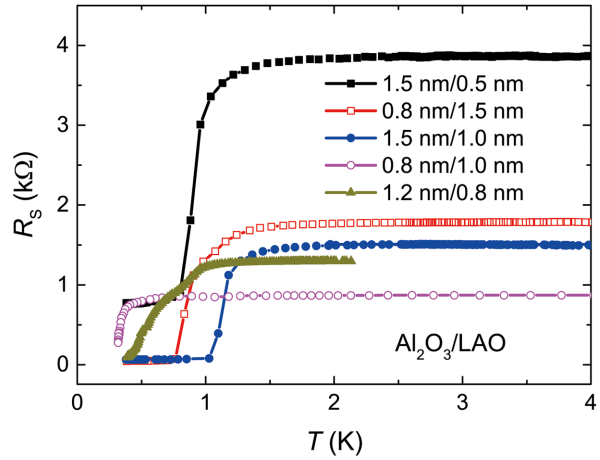

FIG. 4. Low-temperature transport properties of Al_2O_3/LAO/KTO(111) samples. The films on the top of KTO substrates are Al_2O_3/LAO bilayers that were grown subsequently under normal conditions. The thicknesses of the two layers in different samples are as labeled.

prospect to make sketched superconducting nanoelectronics by an AFM tip, with a much higher T_c than that of LAO/STO. Moreover, we present a practical way to reduce the effective critical thickness by a combined deposition of LAO and Al_2O_3, which paves the way to study the interface superconductivity in LAO/KTO(111) by powerful tunneling and spectroscopic techniques.

We thank Y. Zhou for fruitful discussions. This work was supported by the National Key Research and Development Program of China (2017YFA0303002 and 2016YFA0300204), National Natural Science Foundation of China (11934016 and 12074334), the Key R&D Program of Zhejiang Province, China (2020C01019 and 2021C01002), and the Fundamental Research Funds for the Central Universities of China.

[*] To whom correspondence should be addressed.
ywxie@zju.edu.cn

[1] A. Ohtomo and H. Y. Hwang, Nature (London) **427**, 423 (2004).
[2] S. Thiel, G. Hammerl, A. Schmehl, C. W. Schneider, and J. Mannhart, Science **313**, 1942 (2006).
[3] N. Nakagawa, H. Y. Hwang, and D. A. Muller, Nat. Mater. **5**, 204 (2006).
[4] D. G. Schlom and J. Mannhart, Nat. Mater. **10**, 168 (2011).
[5] C. Cen, S. Thiel, J. Mannhart, and J. Levy, Science **323**, 1026 (2009).
[6] G. Cheng, P. F. Siles, F. Bi, C. Cen, D. F. Bogorin, C. W. Bark, C. M. Folkman, J. Park, C. Eom, G. Medeiros-ribeiro, and J. Levy, Nat. Nanotechnol. **6**, 343 (2011).
[7] C. Cen, S. Thiel, G. Hammerl, C. W. Schneider, K. E. Andersen, C. S. Hellberg, J. Mannhart, and J. Levy, Nat. Mater. **7**, 298 (2008).

[8] Y. Xie, C. Bell, T. Yajima, Y. Hikita, and H. Y. Hwang, Nano Lett. **10**, 2588 (2010).
[9] C. Liu, X. Yan, D. Jin, Y. Ma, H.-W. Hsiao, Y. Lin, T. M. Bretz-Sullivan, X. Zhou, J. Pearson, B. Fisher, J. S. Jiang, W. Han, J.-M. Zuo, J. Wen, D. D. Fong, J. Sun, H. Zhou, and A. Bhattacharya, Science **371**, 716 (2021).
[10] Z. Chen, Z. Liu, Y. Sun, X. Chen, Y. Liu, H. Zhang, H. Li, M. Zhang, S. Hong, T. Ren, C. Zhang, H. Tian, Y. Zhou, J. Sun, and Y. Xie, Phys. Rev. Lett. **126**, 026802 (2021).
[11] Y. Ma, J. Niu, W. Xing, Y. Yao, R. Cai, J. Sun, X. C. Xie, X. Lin, and W. Han, Chin. Phys. Lett. **37**, 117401 (2020).
[12] H. Zhang, H. Zhang, X. Yan, X. Zhang, Q. Zhang, J. Zhang, F. Han, L. Gu, B. Liu, Y. Chen, B. Shen, and J. Sun, ACS Appl. Mater. Interfaces **9**, 36456 (2017).
[13] Z. Chen, Y. Liu, H. Zhang, Z. Liu, H. Tian, Y. Sun, M. Zhang, Y. Zhou, J. Sun, and Y. Xie, Science **372**, 721 (2021).
[14] J. R. Thompson, L. A. Boatner, and J. O. Thomson, J. Low Temp. Phys. **47**, 467 (1982).
[15] K. Ueno, S. Nakamura, H. Shimotani, H. T. Yuan, N. Kimura, T. Nojima, H. Aoki, Y. Iwasa, and M. Kawasaki, Nat. Nanotechnol. **6**, 408 (2011).
[16] J. F. Schooley, W. R. Hosler, and M. L. Cohen, Phys. Rev. Lett. **12**, 474 (1964).
[17] See Supplemental Material at http://link.aps.org/supplemental/10.1103/PhysRevLett.127.086804 for materials and methods and Figs. S1–S9.
[18] Y. Chen, N. Pryds, J. E. Kleibeuker, G. Koster, J. Sun, E. Stamate, B. Shen, G. Rijnders, and S. Linderoth, Nano Lett. **11**, 3774 (2011).
[19] Z. Chen, X. Chen, B. Mao, Q. Li, M. Zhang, H. Bo, Z. Liu, H. Tian, Z. Zhang, and Y. Xie, Adv. Mater. Interfaces **5**, 1801216 (2018).
[20] Z. Chen, M. Zhang, T. Ren, and Y. Xie, J. Phys. Condens. Matter **31**, 505002 (2019).
[21] M. Zhang, Z. Chen, B. Mao, Q. Li, H. Bo, T. Ren, P. He, Z. Liu, and Y. Xie, Phys. Rev. Mater. **2**, 065002 (2018).
[22] W. Siemons, G. Koster, H. Yamamoto, W. A. Harrison, G. Lucovsky, T. H. Geballe, D. H. A. Blank, and M. R. Beasley, Phys. Rev. Lett. **98**, 196802 (2007).
[23] M. Salluzzo, S. Gariglio, D. Stornaiuolo, V. Sessi, S. Rusponi, C. Piamonteze, G. M. De Luca, M. Minola, D. Marré, A. Gadaleta, H. Brune, F. Nolting, N. B. Brookes, and G. Ghiringhelli, Phys. Rev. Lett. **111**, 087204 (2013).
[24] Z. Q. Liu, C. J. Li, W. M. Lü, X. H. Huang, Z. Huang, S. W. Zeng, X. P. Qiu, L. S. Huang, A. Annadi, J. S. Chen, J. M. D. Coey, T. Venkatesan, and Ariando, Phys. Rev. X **3**, 021010 (2013).
[25] S. A. Chambers, *Hard X-Ray Photoelectron Spectroscopy (HAXPES)* (Springer, New York, 2016).
[26] L. Yu and A. Zunger, Nat. Commun. **5**, 5118 (2014).
[27] Y. Z. Chen, N. Bovet, T. Kasama, W. W. Gao, S. Yazdi, C. Ma, N. Pryds, and S. Linderoth, Adv. Mater. **26**, 1462 (2014).
[28] K. Yoshimatsu, R. Yasuhara, H. Kumigashira, and M. Oshima, Phys. Rev. Lett. **101**, 026802 (2008).
[29] C. Richter, H. Boschker, W. Dietsche, E. Fillis-Tsirakis, R. Jany, F. Loder, L. F. Kourkoutis, D. A. Muller, J. R. Kirtley, C. W. Schneider, and J. Mannhart, Nature (London) **502**, 528 (2013).
[30] G. Berner, M. Sing, H. Fujiwara, A. Yasui, Y. Saitoh, A. Yamasaki, Y. Nishitani, A. Sekiyama, N. Pavlenko, T. Kopp, C. Richter, J. Mannhart, S. Suga, and R. Claessen, Phys. Rev. Lett. **110**, 247601 (2013).